Mechanistic Characterization of Aerobic Alcohol Oxidation Catalyzed by Pd(OAc) 2 /Pyridine Including Identification of the Catalyst Resting State and the Origin of Nonlinear [Catal...

ARTICLE *in* JOURNAL OF THE AMERICAN CHEMICAL SOCIETY · OCTOBER 2004

Impact Factor: 12.11 · DOI: 10.1021/ja049962m · Source: PubMed

3 AUTHORS, INCLUDING:

Ilia A Guzei
University of Wisconsin–Madison
340 PUBLICATIONS **6,763** CITATIONS

J|A|C|S
ARTICLES
Published on Web 08/21/2004

Mechanistic Characterization of Aerobic Alcohol Oxidation Catalyzed by $Pd(OAc)_2$/Pyridine Including Identification of the Catalyst Resting State and the Origin of Nonlinear [Catalyst] Dependence

Bradley A. Steinhoff, Ilia A. Guzei, and Shannon S. Stahl*

Contribution from the Department of Chemistry, University of Wisconsin-Madison, 1101 University Avenue, Madison, Wisconsin 53706

Received January 2, 2004; E-mail: stahl@chem.wisc.edu

Abstract: The $Pd(OAc)_2$/pyridine catalyst system is one of the most convenient and versatile catalyst systems for selective aerobic oxidation of organic substrates. This report describes the catalytic mechanism of $Pd(OAc)_2$/pyridine-mediated oxidation of benzyl alcohol, which has been studied by gas-uptake kinetic methods and ^{1}H NMR spectroscopy. The data reveal that turnover-limiting substrate oxidation by palladium(II) proceeds by a four-step pathway involving (1) formation of an adduct between the alcohol substrate and the square-planar palladium(II) complex, (2) proton-coupled ligand substitution to generate a palladium-alkoxide species, (3) reversible dissociation of pyridine from palladium(II) to create a three-coordinate intermediate, and (4) irreversible β-hydride elimination to produce benzaldehyde. The catalyst resting state, characterized by ^{1}H NMR spectroscopy, consists of an equilibrium mixture of $(py)_2Pd(OAc)_2$, **1**, and the alcohol adduct of this complex, **1·RCH$_2$OH**. These in situ spectroscopic data provide direct support for the mechanism proposed from kinetic studies. The catalyst displays higher turnover frequency at lower catalyst loading, as revealed by a nonlinear dependence of the rate on [catalyst]. This phenomenon arises from a competition between forward and reverse reaction steps that exhibit unimolecular and bimolecular dependences on [catalyst]. Finally, overoxidation of benzyl alcohol to benzoic acid, even at low levels, contributes to catalyst deactivation by formation of a less active palladium benzoate complex.

Introduction

Homogeneous palladium-catalyzed reactions include two major classes: cross-coupling reactions initiated by palladium(0) (eqs 1 and 2) and oxidation reactions initiated by palladium(II) (eqs 3 and 4).[1] The former, which include well-known Heck, Suzuki, Tsuji−Trost, Buchwald−Hartwig, and related cross-coupling reactions,[2] are among the most effective methods in organic synthesis. Palladium-catalyzed oxidation reactions, highlighted by the industrial Wacker process (eq 5),[3] have also received considerable attention,[1,4,5] but they face several key challenges to more widespread utility and application in organic chemistry.

Palladium oxidation catalysis traditionally requires a stoichiometric secondary oxidant consisting of an organic or transition metal reagent such as benzoquinone or $CuCl_2$.[4,5] These oxidants increase the complexity of the reaction, reduce the atom economy, and complicate product isolation. Palladium complexes compatible with these reaction conditions are quite limited because phosphines and related organic ligands, which have been used extensively in palladium-catalyzed cross-coupling reactions, often degrade rapidly under oxidizing reaction conditions. Therefore, palladium-catalyzed oxidation reactions are often limited to the use of simple palladium salts such as $PdCl_2$ and $Pd(OAc)_2$.

$$\text{R–X + Nu-H + B:} \xrightarrow{\text{[Pd]}} \text{R–Nu + B-H}^+\text{X}^- \quad (1)$$

$$\text{R–X + Nu-M} \xrightarrow{\text{[Pd]}} \text{R–Nu + M-X} \quad (2)$$

$$\text{SubH}_2 + \text{[Ox]} \xrightarrow{\text{[Pd]}} \text{Sub}^{ox} + \text{[Ox]H}_2 \quad (3)$$

$$\text{SubH + Sub'H + [Ox]} \xrightarrow{\text{[Pd]}} \text{Sub–Sub' + [Ox]H}_2 \quad (4)$$

$$\text{CH}_2{=}\text{CH}_2 + 1/2\ \text{O}_2 \xrightarrow{\text{[Pd/Cu]}} \text{H}_3\text{C}(\text{C}{=}\text{O})\text{H} \quad (5)$$

Significant recent developments have begun to address these limitations. An increasing number of reactions employ molecular oxygen as the stoichiometric oxidant, and often no cocatalyst is required for catalyst reoxidation.[6] Moreover, several oxidatively stable ligands have been identified to promote catalytic turnover and improve catalyst stability. These ligands often

(1) Tsuji, J. *Palladium Reagents and Catalysts*; Wiley: New York, 1995.
(2) (a) Diederich, F., Stang, P. J., Eds. *Metal-Catalyzed Cross-Coupling Reactions*; Wiley−VCH: New York, 1998. (b) Beletskaya, I. P.; Cheprakov, A. V. *Chem. Rev.* **2000**, *100*, 3009−3066. (c) Hartwig, J. F. In *Modern Amination Methods*; Ricci, A., Ed.; Wiley−VCH: New York, 2000; pp 195−262. (d) Muci, A. R.; Buchwald, S. L. *Top. Curr. Chem.* **2002**, *219*, 131−209. (e) Trost, B. M.; Van Vranken, D. L. *Chem. Rev.* **1996**, *96*, 395−422.
(3) Jira, R. In *Applied Homogeneous Catalysis with Organometallic Compounds*; Cornils, B., Herrmann, W. A., Eds.; Wiley-VCH: New York, 2002; Vol. 1, pp 386−405.
(4) Henry, P. M. *Palladium Catalyzed Oxidation of Hydrocarbons*; Kluwer: Boston, 1980.
(5) (a) Bäckvall, J.-E. *Acc. Chem. Res.* **1983**, *16*, 335−342. (b) Hosokawa, T.; Murahashi, S.-I. *Acc. Chem. Res.* **1990**, *23*, 49−54.

10.1021/ja049962m CCC: $27.50

consist of nitrogen donors, and the list includes chiral examples, such as (−)-sparteine,[7] that enable enantioselective transformations. These advances are quite promising, but, overall, the reactions remain considerably less effective than palladium-catalyzed cross-coupling reactions.

To provide a rational basis for the development of improved palladium oxidation catalysts, we[8] and others[9−11] have begun investigating the mechanism of palladium-catalyzed reactions that undergo direct dioxygen-coupled turnover. Much of this work has focused on aerobic alcohol oxidation, and the Pd(OAc)$_2$/pyridine catalyst system developed by Uemura and coworkers[12] is among the most effective and convenient catalyst system for this reaction (eq 6). Aliphatic, benzylic, and allylic alcohols are all oxidized efficiently under an ambient pressure of oxygen. Furthermore, very similar catalyst systems have been used in the selective oxidation of other organic substrates, including oxidative ring-cleavage of *tert*-cyclobutanols (eq 7),[13] alkene hetero- and carbocyclizations (eqs 8−9),[7c,14] and intermolecular C−C coupling reactions.[15] This catalytic versatility and prospects for additional applications provide significant motivation to elucidate factors that could improve catalyst activity and lifetime.

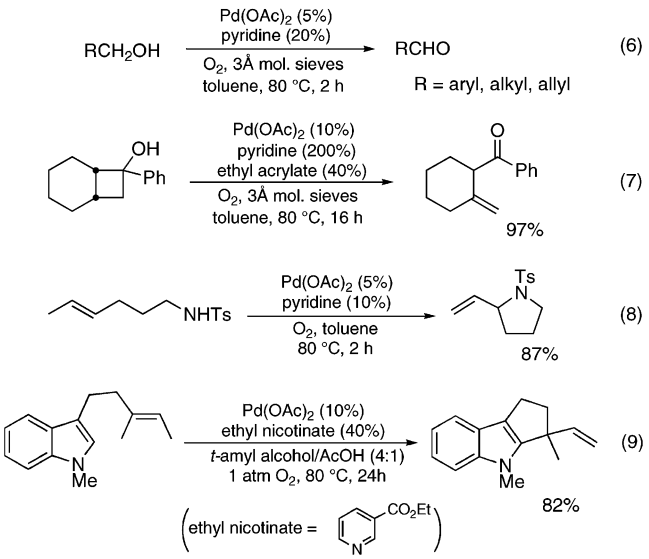

This report provides a systematic mechanistic analysis of the Pd(OAc)$_2$/pyridine-catalyzed aerobic alcohol oxidation of benzyl alcohol. The results provide insights into the role of pyridine as an oxidatively stable ligand and its ability to modulate catalyst stability and activity. The catalyst is more efficient at lower catalyst loading, as revealed by a nonlinear dependence of the rate on catalyst concentration. This behavior has important consequences for new catalyst development, and its mechanistic origin is outlined below. The catalyst resting state has been characterized spectroscopically during catalytic turnover, and its identification provides independent confirmation of the mechanism proposed from kinetics data.[16]

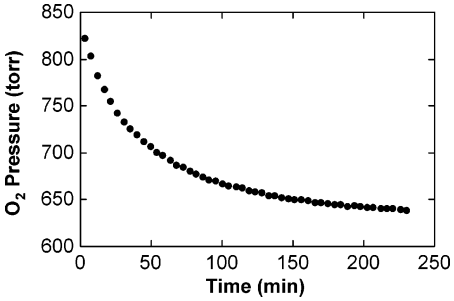

Figure 1. A representative kinetic time-course for the Pd(OAc)$_2$/pyridine-catalyzed oxidation of benzyl alcohol obtained by gas-uptake methods. Data sampling occurred at a rate of 1 s^{-1} (not all data are shown). Conditions: [Pd(OAc)$_2$] = 5.0 mM, [pyridine] = 20 mM, [alcohol] = 0.10 M, 5 mL of toluene, 80 °C.

Results

Kinetics Studies: Substrate and Catalyst Effects. The aerobic oxidation of benzyl alcohol catalyzed by Pd(OAc)$_2$/pyridine (5/20 mol %) (eq 10) proceeds to complete conversion within 4 h at 80 °C. A computer-interfaced gas-uptake apparatus was constructed to acquire kinetics of the catalytic reaction in situ by monitoring the change in oxygen pressure within a sealed, temperature-controlled reaction vessel. The reaction time-course (Figure 1) reveals a monotonic decrease in pressure, and the lack of an induction period enabled us to obtain much of our kinetics data via initial-rates methods.

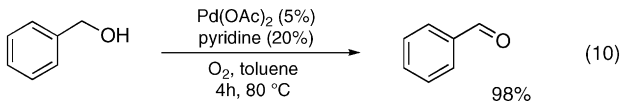

The initial kinetic studies focused on the contribution of primary reaction components (alcohol, O_2, and catalyst) to the catalytic turnover rate (Figures 2−4). These plots reveal a saturation rate dependence on the alcohol and catalyst concentrations and a lack of dependence on the O_2 pressure above 250 Torr. At reduced oxygen pressures, significantly lower turnover rates coincide with observed deposition of catalytically inactive palladium black. Comparison of the rate of benzyl

(6) For a recent review, see: Stahl, S. S. *Angew. Chem., Int. Ed.* **2004**, *43*, 3400−3420.
(7) (a) Jensen, D. R.; Pugsley, J. S.; Sigman, M. S. *J. Am. Chem. Soc.* **2001**, *123*, 7475−7476. (b) Ferreira, E. M.; Stoltz, B. M. *J. Am. Chem. Soc.* **2001**, *123*, 7725−7726. (c) Trend, R. M.; Ramtohul, Y. K.; Ferreira, E. M.; Stoltz, B. M. *Angew. Chem., Int. Ed.* **2003**, *42*, 2892−2895.
(8) (a) Stahl, S. S.; Thorman, J. L.; Nelson, R. C.; Kozee, M. A. *J. Am. Chem. Soc.* **2001**, *123*, 7188−7189. (b) Steinhoff, B. A.; Fix, S. R.; Stahl, S. S. *J. Am. Chem. Soc.* **2002**, *124*, 766−767. (c) Steinhoff, B. A.; Stahl, S. S. *Org. Lett.* **2002**, *4*, 4179−4181. (d) Stahl, S. S.; Thorman, J. L.; de Silva, N.; Guzei, I. A.; Clark, R. W. *J. Am. Chem. Soc.* **2003**, *125*, 12−13.
(9) (a) ten Brink, G.-J.; Arends, I. W. C. E.; Papadogianakis, G.; Sheldon, R. A. *Appl. Catal., A* **2000**, *194*−*195*, 435−442. (b) ten Brink, G.-J.; Arends, I. W. C. E.; Sheldon, R. A. *Adv. Synth. Catal.* **2002**, *344*, 355−369. (c) ten Brink, G.-J.; Arends, I. W. C. E.; Hoogenraad, M.; Verspui, G.; Sheldon, R. A. *Adv. Synth. Catal.* **2003**, *345*, 497−505. (d) ten Brink, G.-J.; Arends, I. W. C. E.; Hoogenraad, M.; Verspui, G.; Sheldon, R. A. *Adv. Synth. Catal.* **2003**, *345*, 1341−1352.
(10) (a) Mueller, J. A.; Jensen, D. R.; Sigman, M. S. *J. Am. Chem. Soc.* **2002**, *124*, 8202−8203. (b) Mueller, J. A.; Sigman, M. S. *J. Am. Chem. Soc.* **2003**, *125*, 7005−7013. (c) Jensen, D. R.; Schultz, M. J.; Mueller, J. A.; Sigman, M. S. *Angew. Chem., Int. Ed.* **2003**, *42*, 3810−3813.
(11) (a) Bianchi, D.; Bortolo, R.; D'Aloisio, R.; Ricci, M. *J. Mol. Catal. A* **1999**, *150*, 87−94. (b) Bianchi, D.; Bortolo, R.; D'Aloisio, R.; Querci, C.; Ricci, M. *Stud. Surf. Sci. Catal.* **1999**, *126*, 481−484. (c) Bortolo, R.; Bianchi, D.; D'Aloisio, R.; Querci, C.; Ricci, M. *J. Mol. Catal. A* **2000**, *153*, 25−29.
(12) (a) Nishimura, T.; Onoue, T.; Ohe, K.; Uemura, S. *Tetrahedron Lett.* **1998**, *39*, 6011−6014. (b) Nishimura, T.; Onoue, T.; Ohe, K.; Uemura, S. *J. Org. Chem.* **1999**, *64*, 6750−6755.
(13) (a) Nishimura, T.; Ohe, K.; Uemura, S. *J. Org. Chem.* **2001**, *66*, 1455−1465. (b) Nishimura, T.; Ohe, K.; Uemura, S. *J. Am. Chem. Soc.* **1999**, *121*, 2645−2646. (c) Park, S.-B.; Cha, J. K. *Org. Lett.* **2000**, *2*, 147−149.
(14) (a) Fix, S. R.; Brice, J. L.; Stahl, S. S. *Angew. Chem., Int. Ed.* **2002**, *41*, 164−166. (b) Ferreira, E. M.; Stoltz, B. M. *J. Am. Chem. Soc.* **2003**, *125*, 9578−9579.
(15) Nishimura, T.; Araki, H.; Maeda, Y.; Uemura, S. *Org. Lett.* **2003**, *5*, 2997−2999.
(16) For a preliminary report on the kinetics of this catalyst system, see ref 8c.

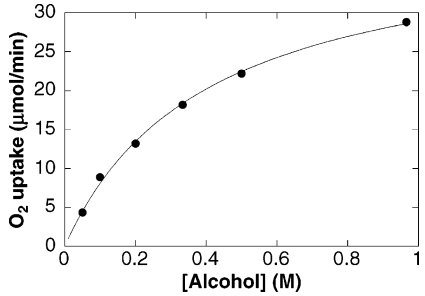

Figure 2. Dependence of the initial rate on alcohol concentration. The curve fit results from a nonlinear least-squares fit to a hyperbolic function of [alcohol] (eq 16). Conditions: $[Pd(OAc)_2] = 5.0$ mM, [pyridine] = 20 mM, [alcohol] = 0.05−0.97 M, initial $pO_2 = 700$ Torr, 10 mL of toluene, 80 °C.

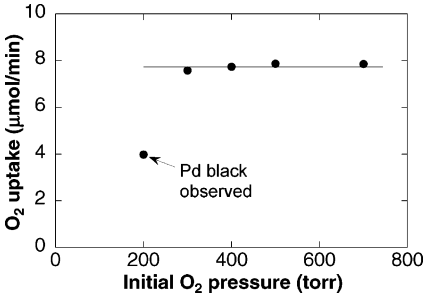

Figure 3. Dependence of the initial rate on the initial oxygen pressure. Conditions: $[Pd(OAc)_2] = 5.0$ mM, [pyridine] = 20 mM, [alcohol] = 0.10 M, initial $pO_2 = 200-700$ Torr, 10 mL of toluene, 80 °C.

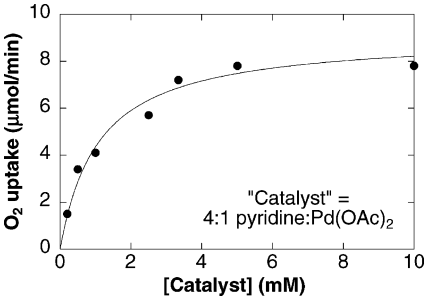

Figure 4. Dependence of the initial rate on catalyst concentration, where the "catalyst" is a 4:1 mixture of pyridine and $Pd(OAc)_2$. The curve fit reflects a nonlinear least-squares fit to a generic hyperbolic function of [catalyst]: rate = C_1[catalyst]/(C_2 + C_3[catalyst]). Conditions: $[Pd(OAc)_2]$ = 0.20−10 mM, [pyridine] = 0.8−40 mM, [alcohol] = 0.10 M, initial $pO_2 = 700$ Torr, 10 mL of toluene, 80 °C.

alcohol oxidation with that of $PhCD_2OH$ reveals a deuterium kinetic isotope effect (KIE) of 1.5(3).[17] This value is substantially attenuated relative to the intrinsic KIE obtained by a competition experiment with PhCHDOH as the substrate: $k_H/k_D = 2.6(2)$.

Kinetics Studies: Pyridine, Acetate, and Acetic Acid Effects. The initial turnover rates exhibit a sharp dependence on [pyridine] that maximizes at a py:Pd ratio of 1:1 (Figure 5). The rate is strongly inhibited at increased [pyridine]; however, the catalyst is also more stable. At py:Pd ratios below 4:1, catalytic turnover is accompanied by significant palladium black deposition and reduced substrate conversion. At a py:Pd ratio of 100:1, the rate is quite slow, but no catalyst decomposition is observed even at very low oxygen pressures (<200 Torr) (Figure S1; cf. Figure 3). The catalyst composition of 4:1 py:Pd optimized by Uemura for synthetic applications appears to reflect a balance between optimal turnover rate and catalyst stability.

(17) We reported previously (ref 8c) that the deuterium kinetic isotope effect varies with [alcohol]: $k_H/k_D = 1.3(2)$ and 1.8(1) at [alcohol] = 0.10 and 1.0 M, respectively. Reinvestigation of these studies revealed the following new and revised deuterium kinetic isotope effects (relative turnover rates for $PhCH_2OH$ and $PhCD_2OH$): $k_H/k_D = 1.6(2)$, 1.4(2), and 1.6(2) at [alcohol] = 0.05, 0.10, and 1.0 M, respectively. The latter two values fall within the uncertainty of the originally reported KIEs, but inclusion of the 0.05 M data forces us to conclude that the KIE does not depend on [alcohol].

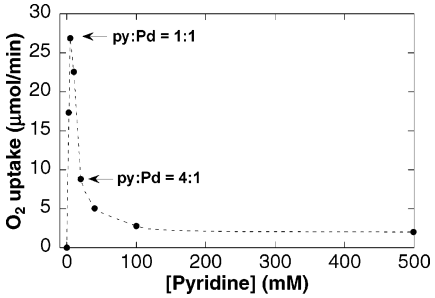

Figure 5. Dependence of the initial rate on pyridine concentration with the $[Pd(OAc)_2]$ held constant. Conditions: $[Pd(OAc)_2] = 5.0$ mM, [pyridine] = 0−500 mM, [alcohol] = 0.10 M, initial $pO_2 = 700$ Torr, 10 mL of toluene, 80 °C.

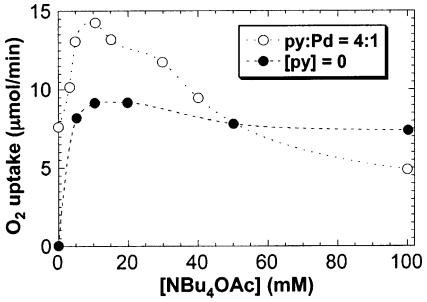

Figure 6. Dependence of the initial rate on NBu_4OAc concentration when the reaction is conducted in the presence (○) or absence (●) of pyridine. Conditions: $[Pd(OAc)_2] = 5.0$ mM, [pyridine] = 20 mM, [alcohol] = 0.10 M, [NBu_4OAc] = 0−100 mM, initial $pO_2 = 700$ Torr, 10 mL of toluene, 80 °C (○); $[Pd(OAc)_2] = 5.0$ mM, [pyridine] = 0 mM, [alcohol] = 0.10 M, [NBu_4OAc] = 0−100 mM, initial $pO_2 = 700$ Torr, 5 mL of toluene, 80 °C (●).

In the absence of pyridine, no catalytic turnover is observed during the initial-rate time period (Figure 5, [py] = 0). Stoichiometric oxidation of benzyl alcohol by $Pd(OAc)_2$ occurs with concomitant formation of palladium black. Catalytic turnover in the absence of pyridine can be achieved by including catalytic quantities of NBu_4OAc in the reaction (Figure 6, ●). Optimal results are obtained when both exogenous acetate and pyridine are present in the reaction mixture (Figure 6, ○). A nearly 2-fold increase in the rate can be achieved by adding 10 mol % NBu_4OAc to the standard catalyst mixture (pyridine:NBu_4OAc:$Pd(OAc)_2$ = 4:2:1). Crystals that formed upon cooling a catalytic reaction mixture containing NBu_4OAc provide a possible explanation for the beneficial effect of acetate. Single-crystal X-ray diffraction analysis of these crystals revealed an adduct between acetic acid and acetate, $NBu_4[AcOH\cdots OAc]^-$ (**2**, Figure S15).[18] Acetic acid, expected as a

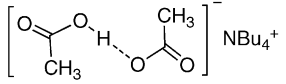

2

byproduct in the equilibrium formation of a palladium alkoxide (eq 11), will be stabilized by formation of an acid−base complex

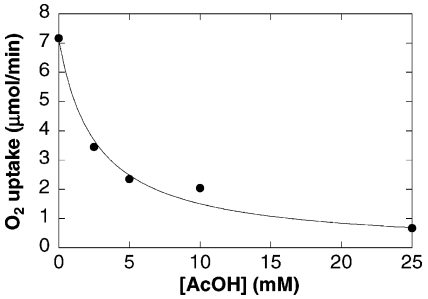

Figure 7. Dependence of the initial rate on acetic acid concentration. The curve fit results from a nonlinear least-squares fit to eq 16. Conditions: $[Pd(OAc)_2] = 5.0$ mM, [pyridine] = 20 mM, [alcohol] = 0.10 M, [AcOH] = 0−25 mM, initial $pO_2 = 700$ Torr, 10 mL of toluene, 80 °C.

(hydrogen-bonding interaction) between acetate and acetic acid. At elevated [NBu_4OAc] (>10 mM), the dropoff in catalytic rate correlates with ^{1}H NMR spectroscopic detection of anionic palladium(II) complexes, $[Pd(py)_{4-n}(OAc)_n]^{(n-2)-}$ ($n = 3$, 4), that arise from displacement of pyridine by acetate. This correlation suggests anionic complexes are less active catalysts for alcohol oxidation. Addition of acetic acid to the reaction mixture significantly suppresses the turnover rate (Figure 7).

$$L_nPd{-}OAc + RCH_2OH \rightleftharpoons L_nPd{-}OCH_2R + AcOH \quad (11)$$

Rate Dependence on Catalyst Concentration: Linear and Nonlinear Behavior. If [pyridine] is held constant while [$Pd(OAc)_2$] is varied (py:Pd = 12.5−250), the plot of initial rates reveals a square-root dependence on [$Pd(OAc)_2$] (Figure 8A). This result contrasts the hyperbolic dependence observed when the catalyst concentration is varied at a constant py:Pd ratio of 4:1 (Figure 4). The rate dependence on [$Pd(OAc)_2$] changes again when both pyridine and acetic acid are added to the reaction mixture (80 and 5 mM, respectively); under these conditions, a linear dependence is observed (Figure 8B).

In Situ Characterization of the Catalyst Resting State and Identification of a Catalyst Deactivation Pathway. ^{1}H NMR spectroscopic studies were conducted to gain insights into the palladium speciation under catalytic conditions. Addition of 2 equiv of pyridine to $Pd(OAc)_2$ in toluene-d_8 at 80 °C reveals a spectrum of the known complex, *trans*-$(py)_2Pd(OAc)_2$ (**1**).[19] If more than 2 equiv of pyridine are added, two sets of pyridine resonances are observed, which correspond to coordinated and free pyridine. Integration data reveal that only 2 equiv of pyridine coordinates to palladium, even in the presence of up to 50 equiv of pyridine.

Addition of benzyl alcohol to a solution of the catalyst (1:4 $Pd(OAc)_2$:py) in toluene-d_8 alters the chemical shifts of both coordinated and free pyridine in the ^{1}H NMR spectrum (Figure 9A, pyridine ortho C−H shifts; Figures S2−S3, full spectra). Shifts in the free pyridine resonances are unaffected by the presence of the palladium complex. At lower temperatures (<25 °C), the effects of added alcohol can be studied without the complication of competing alcohol oxidation. The changes in chemical shift exhibit a saturation dependence on the alcohol concentration, and this effect has been examined for benzyl alcohol and two analogues, *para*-chloro- and *para*-methoxybenyzl alcohol. (Figures 9B and S4−S5). Hydrogen bonding between pyridine and alcohol can account for the chemical shift changes of free pyridine. Coordinated pyridine, however, does not have a lone pair available for hydrogen bonding, and changes in its chemical shift must have a different origin. Several possibilities may be considered: (1) rapid equilibrium formation of a palladium alkoxide complex, (2) equilibrium coordination of the alcohol to palladium forming a five-coordinate adduct, or (3) hydrogen-bonding interactions between the alcohol and the acetate ligands. Integration of the coordinated pyridine and acetate resonances reveals both ligands are present in a 2:1 ratio relative to palladium, even at high [alcohol]. Equilibrium formation of a palladium alkoxide, which would occur with concomitant release of acetic acid (eq 11), is inconsistent with this result. The lack of new resonances for the alcohol substrate, even at low temperature, indicates that equilibrium formation of an adduct between **1** and $PhCH_2OH$, generically formulated as **1·RCH$_2$OH**, undergoes rapid exchange. The precise nature of this interaction cannot be discerned from the available data, but two reasonable possibilities include alcohol coordination to the palladium(II) center or hydrogen bonding between the alcohol and the uncoordinated carbonyl oxygen of an acetate ligand (see discussion below).

Formation of **1·RCH$_2$OH** is favored at moderate alcohol concentrations (Figure 9B). By assuming a simple equilibrium binding model, we have determined the equilibrium constants at 22 °C for all three alcohol substrates (eq 12, Table S1). The equilibrium constants for the different alcohols exhibit a linear Hammett relationship ($\rho = +0.37$, Figure S6) that reveals alcohols bearing electron-withdrawing groups (i.e., more acidic alcohols) bind more tightly. The interaction between benzyl alcohol and $(py)_2Pd(OAc)_2$ was investigated over a 100 °C temperature range (−75 to 25 °C), and van't Hoff analysis of the equilibrium constants (Figure S7) enabled the determination of thermodynamic parameters for binding: $\Delta H = -1.4(2)$ kcal/mol, $\Delta S = -0.4(7)$ eu. Extrapolation of the data to 80 °C reveals the equilibrium constant for formation of **1·RCH$_2$OH** is 6.3 M^{-1} under catalytic conditions.

$$\underset{\mathbf{1}}{(py)_2Pd(OAc)_2} + RCH_2OH \overset{K_{12}}{\rightleftharpoons} \underset{\mathbf{1{\cdot}RCH_2OH}}{[(py)_2Pd(OAc)_2]{\cdot}RCH_2OH} \quad (12)$$

RCH_2OH	K_{12} (M^{-1}, 22 °C)
p-$ClC_6H_4CH_2OH$	11.5
$C_6H_5CH_2OH$	9.2
p-$MeOC_6H_4CH_2OH$	7.4

High pressures of oxygen gas (10 atm) were required to monitor the catalytic reaction in situ by ^{1}H NMR spectroscopy. Gas−liquid mixing in an unstirred NMR tube is inefficient, and the elevated gas pressure is necessary to prevent catalyst decomposition during the course of the reaction. The quantity of dissolved oxygen at ambient pressure is too low (~10 mM in toluene at 80 °C)[20] to permit complete substrate conversion.

(18) For previous characterization of related structures, see: (a) Nahringbauer, I. *Acta Chem. Scand.* **1969**, *23*, 1653−1666. (b) Darensbourg, D. J.; Longridge, E. M.; Atnip, E. V.; Reibenspies, J. H. *Inorg. Chem.* **1992**, *31*, 3951−3955. (c) Li, Q.; Mak, T. C. W. *J. Inclusion Phenom. Mol. Recognit. Chem.* **1997**, *28*, 183−204.

(19) (a) For crystallographic characterization, see: Kravtsova, S. V.; Romm, I. P.; Stash, A. I.; Belsky, V. K. *Acta Crystallogr., Sect. C* **1996**, *52*, 2201−2204. (b) ^{1}H NMR spectroscopic characterization: Schultz, M. J.; Park, C. C.; Sigman, M. S. *Chem. Commun.* **2002**, 3034−3035.

(20) (a) Battino, R., Ed. *Solubility Data Series, Vol. 7: Oxygen and Ozone*; Pergamon: New York, 1981. (b) Fischer, K.; Wilken, M. *J. Chem. Thermodyn.* **2001**, *33*, 1285−1308.

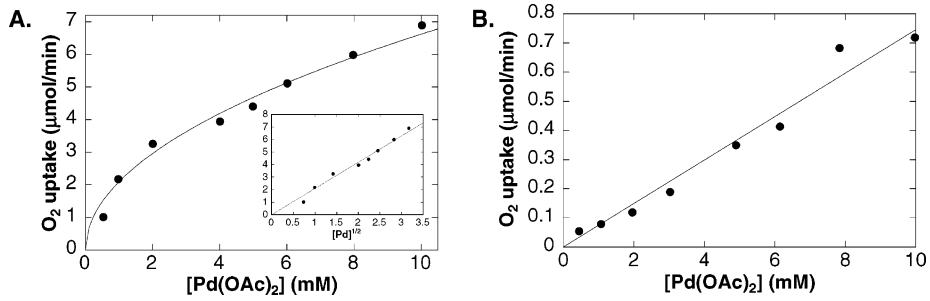

Figure 8. Dependence of the initial rate on $Pd(OAc)_2$ concentration in the presence of a large excess of pyridine (py:Pd ≥ 12.5) (A) and the in the presence of added acetic acid (5 mM) and a large excess of pyridine (py:Pd ≥ 8) (B). The curve in (A) is derived from a nonlinear least-squares fit to the square-root function of $[Pd(OAc)_2]$. The curve fit in (B) reflects a linear least-squares fit to the data. Conditions: (A) $[Pd(OAc)_2] = 0.45-10.0$ mM, [pyridine] = 125 mM, [alcohol] = 0.10 M, initial pO_2 = 700 Torr, 10 mL of toluene, 80 °C. (B) $[Pd(OAc)_2] = 0.45-10$ mM, [pyridine] = 80 mM, [alcohol] = 0.10 M, [AcOH] = 5.0 mM, initial pO_2 = 700 Torr, 5 mL of toluene, 80 °C.

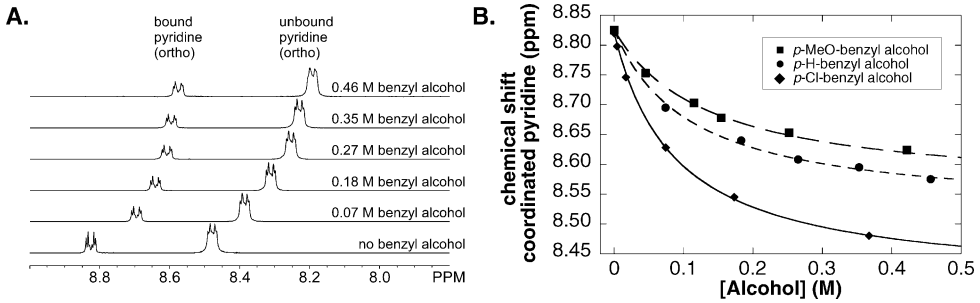

Figure 9. (A) Changes in the pyridine chemical shifts with added benzyl alcohol. Conditions: $[Pd(OAc)_2] = 2.2$ mM, [pyridine] = 15.1 mM, [benzyl alcohol] = 0−460 mM, toluene-d_8, 22 °C. (B) Effect of different alcohols on the chemical shift (ortho C−H) of coordinated pyridine in toluene-d_8 at 22 °C. The alcohols include 4-methoxybenzyl alcohol (■), benzyl alcohol (●), and 4-chlorobenzyl alcohol (◆). Conditions: (i) $[Pd(OAc)_2] = 2.5$ mM, [pyridine] = 18.8 mM, [4-methoxybenzyl alcohol] = 0−420 mM. (ii) $[Pd(OAc)_2] = 2.2$ mM, [pyridine] = 15.1 mM, [benzyl alcohol] = 0−460 mM. (iii) $[Pd(OAc)_2] = 2.7$ mM, [pyridine] = 12.9 mM, [4-chlorobenzyl alcohol] = 0−370 mM. Internal standard = 1,3,5-tri-*tert*-butylbenzene. Chemical shifts for coordinated acetate also display a dependence on the concentration of added alcohol (Figure S5), and the curve fits were obtained by simultaneous nonlinear least-squares fitting of both pyridine (ortho C−H) and acetate data to the equilibrium binding expression in eq S13.

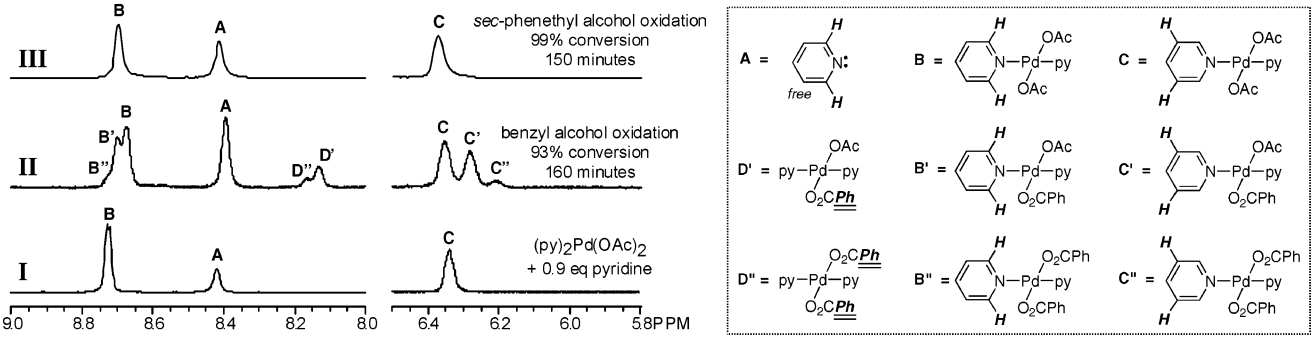

Figure 10. Comparison of the ^1H NMR spectra of $Pd(OAc)_2$/pyridine in toluene (I) and catalytic reaction mixtures from the aerobic oxidation of benzyl alcohol (II) and *sec*-phenethyl alcohol (III). Full spectra of the catalytic reactions at several different time-points are provided in the Supporting Information. Conditions: (I) $[Pd(OAc)_2] = 4.8$ mM, [pyridine] = 14.0 mM, [1,3,5-tri-*tert*-butylbenzene] = 2.9 mM, pO_2 = 10 atm, 0.6 mL of toluene-d_8, 80 °C; (II) $[Pd(OAc)_2] = 5.1$ mM, [pyridine] = 16.8 mM, [alcohol] = 140 mM, [1,3,5-tri-*tert*-butylbenzene] = 3.0 mM, pO_2 = 10 atm, 0.6 mL of toluene-d_8, 80 °C; (III) $[Pd(OAc)_2] = 4.5$ mM, [pyridine] = 15.3 mM, [alcohol] = 150 mM, [1,3,5-tri-*tert*-butylbenzene] = 2.6 mM, pO_2 = 10 atm, 0.6 mL of toluene-d_8, 80 °C.

Oxidation of benzyl alcohol to benzaldehyde, monitored under these conditions, proceeds at a rate predicted by the gas-uptake kinetic studies. The NMR data reveal clean conversion of benzyl alcohol to benzaldehyde, together with a small amount (2.2%) of the overoxidation product, benzoic acid (eq 13). Pyridine is stable under the reaction conditions. Integration of coordinated and free pyridine remains constant throughout the reaction, and possible decomposition products, such as pyridine-*N*-oxide, are not observed.

$$PhCH_2OH \xrightarrow{[O]} PhCHO \xrightarrow{[O]} PhCO_2H \qquad (13)$$

At early time points, the rapidly equilibrating mixture of **1** and **1·RCH$_2$OH** is the only palladium species apparent in solution. As the reaction progresses, however, two new sets of coordinated-pyridine resonances begin to appear (Figure 10,II; for full spectral data, see Figure S8). These resonances correspond to $(py)_2Pd(OAc)(O_2CPh)$ (**3**) and $(py)_2Pd(O_2CPh)_2$ (**4**), which arise from the proton-coupled anionic ligand exchange of benzoate for acetate (eqs 14 and 15). These spectra can be reproduced by simple titration of benzoic acid into a solution of $(py)_2Pd(OAc)_2$.[21] The structure of **4** was also confirmed by X-ray crystallography (Figure S16). Determination of equilibrium constants for eqs 14 and 15 ($K_{14} = 9.3$, $K_{15} = 3.5$; Figure

(21) Small differences between the chemical shifts of **3** and **4**, prepared independently, and those observed under catalytic conditions suggest that a rapidly equilibrating interaction also exists between the alcohol substrate and complexes **3** and **4**.

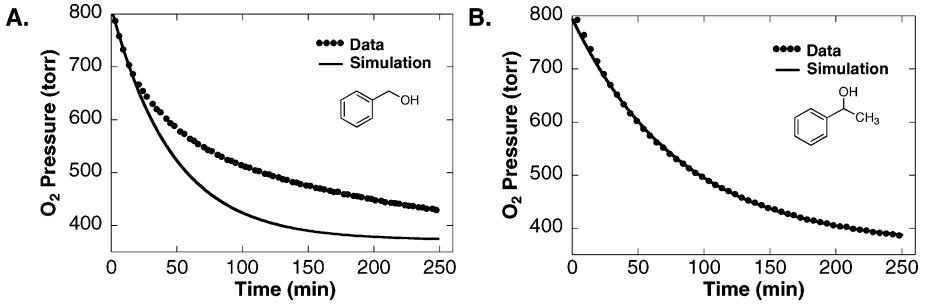

Figure 11. Kinetic time-courses for the aerobic oxidation of benzyl alcohol (A) and *sec*-phenethyl alcohol (B). The simulation is an exponential decay curve derived from the initial rate of the reactions. Deviations between the observed and simulated curves arise from catalyst deactivation or decomposition. Conditions: $[Pd(OAc)_2] = 5.0$ mM, [pyridine] = 20 mM, [alcohol] = 0.25 M, initial $pO_2 = 800$ Torr, 5 mL of toluene, 80 °C.

S9) reveals that benzoate coordinates in preference to acetate. The complexes **1**, **3**, and **4** account for all of the palladium (>95%) in the catalytic reaction, based on integration relative to an internal standard (1,3,5-tri-*tert*-butylbenzene).

$$\underset{\mathbf{1}}{(py)_2Pd(OAc)_2} + PhCO_2H \overset{K_{14}=9.3}{\rightleftharpoons} \underset{\mathbf{3}}{(py)_2Pd(OAc)(O_2CPh)} + AcOH \quad (14)$$

$$\underset{\mathbf{3}}{(py)_2Pd(OAc)(O_2CPh)} + PhCO_2H \overset{K_{15}=3.5}{\rightleftharpoons} \underset{\mathbf{4}}{(py)_2Pd(O_2CPh)_2} + AcOH \quad (15)$$

The catalytic oxidation of *sec*-phenethyl alcohol, PhC(H)(OH)CH_3, was also investigated by ^{1}H NMR spectroscopy because this substrate cannot undergo overoxidation to the carboxylic acid. When this reaction is monitored in situ, **1** is the only palladium species observed throughout the reaction (Figures 10,III and S10). The altered chemical shift of **1** under these catalytic conditions suggests a rapidly equilibrating interaction also takes place between **1** and *sec*-phenethyl alcohol.

Detection and characterization of the palladium(II)−benzoate complexes provides an explanation for catalyst deactivation during the aerobic oxidation of benzyl alcohol. The reaction time-course obtained from gas-uptake measurements indicates that the rate of alcohol oxidation decreases more rapidly than expected (Figure 11A). The simulated curve (solid line, Figure 11A) reflects the expected exponential decay curve derived from the initial turnover rate. The difference between observed and simulated decay curves in this plot arises from the lower catalytic activity of palladium benzoate complexes, **3** and **4**, which form during the reaction. Indeed, $(py)_2Pd(O_2CPh)_2$ (**4**), prepared independently, exhibits a 6-fold lower activity than $(py)_2Pd(OAc)_2$ in the oxidation of benzyl alcohol. In situ formation of **3** and **4** during catalysis also releases acetic acid (eqs 14 and 15), which is known to inhibit catalytic turnover (Figure 7). These results contrast the oxidation of *sec*-phenethyl alcohol, which does not produce carboxylic acid byproduct in the reaction. The correlation between the simulated and experimental decay curve is consistent with the lack of catalyst deactivation (Figure 11B).

Kinetics Studies: Electronic Effects. A series of *para*-substituted benzyl alcohols, $X-C_6H_4CH_2OH$ (X = NO_2, Cl, H, Me, OMe), and pyridines $X-C_5H_4N$ (X = CN, CO_2Me, H, Me, OMe) were used to investigate electronic effects on the catalytic turnover rate. Each of the alcohol substrates exhibits a saturation rate dependence (Figure S11) analogous to that for benzyl alcohol (Figure 2). Electron-rich substrates (X = H, Me, OMe) react more rapidly than those bearing electron-withdrawing groups (X = Cl, NO_2), but Hammett plots derived from rates at a defined alcohol concentration exhibit significant scatter (Figures S12−S13). Pyridine substituent effects, however, follow a systematic trend, and the Hammett plot (Figure 12, $\rho = +0.47$) reveals electron-deficient analogues promote more rapid turnover rates.

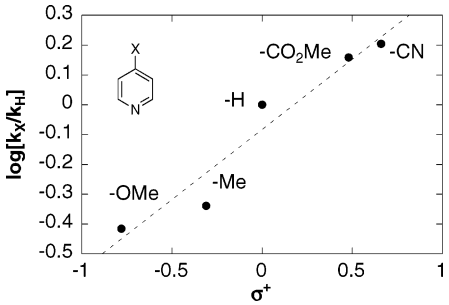

Figure 12. Hammett plot derived from the relative initial rates of catalytic alcohol oxidation conducted with a series of *para*-substituted pyridines. Conditions: $[Pd(OAc)_2] = 5.0$ mM, [pyridine] = 20 mM, [alcohol] = 0.10 M, initial $pO_2 = 700$ Torr, 5 mL of toluene, 80 °C.

Scheme 1. Simplified Catalytic Cycle Displaying the Two-Stage Oxidase Sequence with Competitive Catalyst Decomposition

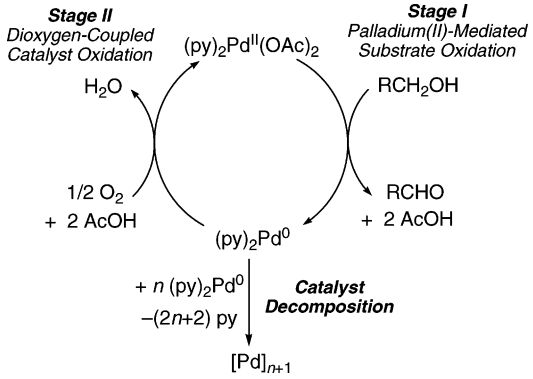

Discussion

Catalytic Mechanism: Overview. Aerobic alcohol oxidation catalyzed by the $Pd(OAc)_2$/pyridine catalyst system proceeds by an oxidase-style mechanism in which palladium(II)-mediated substrate oxidation and aerobic oxidation of the catalyst occur in two independent, sequential stages (Scheme 1).[6] Molecular oxygen is not directly involved in substrate oxidation. Consistent

Scheme 2. Aerobic Oxidation Pathway for a Nitrogen-Coordinated Palladium(0) Complex[8a]

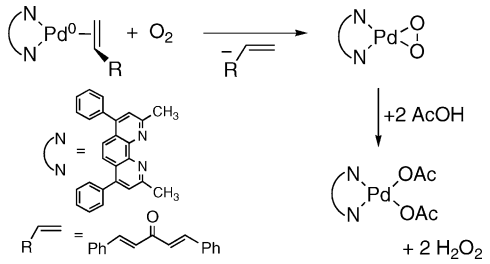

with this proposal, $(py)_2Pd(OAc)_2$ promotes kinetically competent stoichiometric substrate oxidation in the absence of molecular oxygen.

Kinetic studies of the catalytic reaction, which reveal a catalytic rate dependence on catalyst and alcohol concentration, indicate that substrate oxidation (Stage I, Scheme 1) is the turnover-limiting stage of the mechanism. This conclusion finds strong support from the in situ spectroscopic detection of a palladium(II) catalyst resting state, which consists of an equilibrium mixture between *trans*-$(py)_2Pd(OAc)_2$ (**1**) and an alcohol adduct, **1·RCH$_2$OH**. To our knowledge, this is the first time an aerobic palladium oxidation catalyst has been characterized directly during catalytic turnover.

The catalyst oxidation step (Stage II, Scheme 1) is kinetically invisible. Therefore, we cannot evaluate the two principle mechanistic proposals for this stage of the mechanism: oxygen insertion into a palladium(II)-hydride[12b] and oxygenation of ligand-stabilized palladium(0).[8a,c] We favor the latter pathway based on our recent work on the oxygenation of a nitrogen-coordinated palladium(0) complex (Scheme 2).[8a] Attempts to slow the catalyst reoxidation step by lowering the oxygen pressure were unsuccessful because the catalyst undergoes competitive decomposition under these conditions (Figure 3). This observation can be explained by the competition between oxygenation and decomposition of the palladium(0) catalytic intermediate (Scheme 1).

Mechanistic studies of several other catalyst systems have been reported recently.[8b,9−11] Particularly noteworthy are the detailed studies by Sheldon on the aqueous $Pd(OAc)_2$/bathophenanthroline sulfonate (**5**) system[9,22] and by Sigman on asymmetric $PdCl_2$/(−)-sparteine (**6**)-catalyzed alcohol oxidation.[10a,b] Both of these catalysts employ nitrogen donor ligands, and both reactions exhibit turnover-limiting substrate oxidation (Stage I, Scheme 1). The $Pd(OAc)_2$/DMSO catalyst system, studied recently in our laboratory,[8b] is a rare example of a reaction that exhibits turnover-limiting aerobic oxidation of the catalyst (Stage II, Scheme 1). Numerous factors contribute to the rates of individual catalytic steps, but it is reasonable to conclude from these results that the relatively hard nitrogen donor ligands play an important role in enhancing the rate of catalyst oxidation. These reactions generally exhibit high catalyst

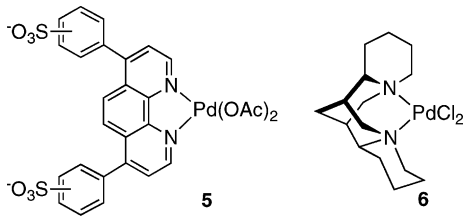

Scheme 3. Stepwise Mechanism for Alcohol Oxidation by $(py)_2Pd(OAc)_2$

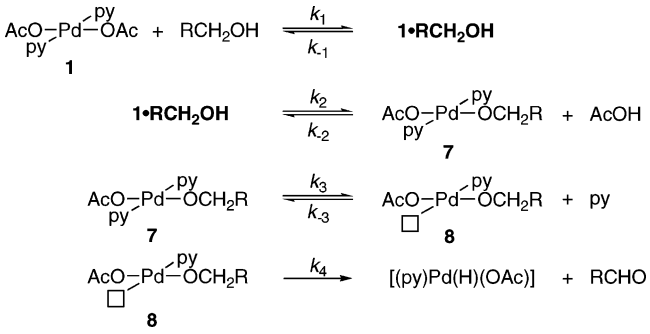

Chart 1. Possible Structures for **1·RCH$_2$OH**

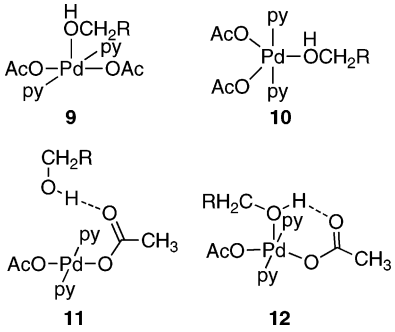

stability because they have a palladium(II) catalyst resting state, which is less prone to decompose by aggregation into palladium black.

Catalytic Mechanism: Details of Palladium(II)-Mediated Alcohol Oxidation. The kinetic results and spectroscopic data provide specific insights into the mechanism of $(py)_2Pd(OAc)_2$-mediated alcohol oxidation. The nonlinear rate dependence on both [alcohol] and [catalyst] (Figures 2 and 4) implicates a multistep pathway, and the data require a mechanism with at least four steps (Scheme 3). This stepwise mechanism begins with a reaction between the alcohol substrate and the palladium(II) catalyst to form an adduct, **1·RCH$_2$OH**, whose identity will be discussed below. This adduct undergoes endergonic conversion to a palladium(II)-alkoxide, **7**, together with the release of acetic acid. This two-step acetate−alkoxide exchange sequence represents a net proton-coupled ligand substitution reaction. Dissociation of pyridine from **7** generates a three-coordinate palladium(II) complex, **8**, that can undergo irreversible β-hydride elimination to yield the aldehyde (or ketone) product.

The first step in this mechanism, formation of adduct **1·RCH$_2$OH**, underlies the saturation kinetic dependence on the alcohol substrate (Figure 2). At sufficiently high [RCH_2OH], with a magnitude defined by the equilibrium constant K_1, the resting state of the catalyst will exist exclusively as **1·RCH$_2$OH**. Higher alcohol concentrations will confer no incremental benefit to the turnover rate.

The precise structure of this adduct is not known, but several reasonable possibilities can be proposed (Chart 1). Structures **9** and **10** represent five-coordinate complexes analogous to those proposed as intermediates in palladium(II) ligand substitution reactions.[23] Despite the logical appeal of these proposed

(22) (a) ten Brink, G.-J.; Arends, I. W. C. E.; Sheldon, R. A. *Science* **2000**, *287*, 1636−1639. (b) Sheldon, R. A.; Arends, I. W. C. E.; ten Brink, G.-J.; Dijksman, A. *Acc. Chem. Res.* **2002**, *35*, 774−781.

structures, our spectroscopic data provide no direct support for such a structure.[24] Several additional factors also require consideration. Structurally characterized examples of five-coordinate palladium(II) complexes generally possess at least one strong π-acceptor ligand,[25] but the ligands in **9** and **10** are exclusively σ (and π) donors. Intermediates in ligand substitution reactions are seldom observed directly, and recent computational studies suggest five-coordinate intermediates may not even form along the reaction coordinate for ligand substitution at d^8, square-planar metal centers.[26]

These considerations suggest the hydrogen-bond adduct, **11**, or the hybrid hydrogen-bonded/five-coordinate adduct, **12**, may represent viable structures for **1·RCH$_2$OH**. Preliminary density-functional-theory (DFT) calculations[27,28] indicate that the hydrogen-bonded structure, **11**, is the only stable intermediate along the reaction pathway between palladium complexes **1** and **7** (Scheme 3, steps 1 and 2). Adduct **11** evolves along the reaction coordinate toward a transition state with a structure resembling **12**, but no other intermediates have been identified. Use of a nonpolar solvent such as toluene will promote hydrogen-bond formation, and this structure can readily account for the highly fluxional behavior of this species. The study of three different *para*-substituted benzyl alcohols indicates that more acidic alcohols bind more tightly. This trend matches that expected for hydrogen-bond donor strength (cf. the effect of these alcohols on the chemical shift of free pyridine, Figure S4). Thermodynamic parameters for K_1 reveal equilibrium formation of **1·RCH$_2$OH** is nearly thermoneutral. This result also seems consistent with proposed structure **11** because interaction between benzyl alcohol and **1** must compete with hydrogen bonding between 2 or more equiv of alcohol. On the basis of these observations, we favor **11** as the structure for **1·RCH$_2$OH**, but definitive assignment must await further study.

The magnitude of the equilibrium constant for formation of the palladium alkoxide, **7**, from a mixture of **1** and PhCH$_2$OH ($K' = K_1 \cdot K_2$, Scheme 3) must be less than ~0.01 based on the inability to detect this complex by ^{1}H NMR spectroscopy under the reaction conditions. This equilibrium constant describes the relative preference of acetate and alkoxide ligands to coordinate to palladium versus a proton. The alkoxide ligand is substantially more basic and prefers to be protonated. Analogous behavior is detected directly in the equilibrium exchange between acetate and benzoate ligands (eqs 14 and 15, Figure S9), in which case protonation of the more basic acetate anion is preferred. This analysis reveals that deactivation of the catalyst upon over-oxidation of benzyl alcohol to benzoic acid and the lower catalytic activity of the (py)$_2$Pd(O$_2$CPh)$_2$ catalyst arise from less favorable equilibrium formation of the palladium alkoxide.

The beneficial effect of added acetate (Figure 6) and inhibition by acetic acid (Figure 7) both reflect the influence of these reagents on equilibrium formation of the alkoxide, **7** ($K_1 \cdot K_2$, Scheme 3). Acetic acid appears on the right side of this equilibrium and, if added, will shift the equilibrium to the left. Acetate does not appear in the equilibrium, and therefore its role is less obvious. Yet exogenous acetate can promote formation of the alkoxide **7** by stabilizing the acetic acid byproduct, essentially serving as a "buffer" to create a more basic reaction medium. The crystallographically characterized [AcOH···OAc]$^-$ adduct (**2**) obtained from the catalytic reaction mixture provides a structural model for this interaction.

The work of Sigman and Stoltz revealed exogenous base is required in alcohol oxidation mediated by [(−)-sparteine]PdCl$_2$ (**6**).[7a,b,29] On the basis of subsequent mechanistic studies, Sigman and co-workers[10] propose that the base is required to deprotonate a coordinated alcohol.[30] In the absence of exogenous base, formation of the palladium alkoxide would require expulsion of HCl, and the thermodynamics of this process are probably sufficiently uphill to prevent substrate oxidation. Relative to chloride, acetate increases the thermodynamic driving force for alcohol deprotonation, and it also provides a kinetically facile pathway for deprotonation via a six-membered transition state resembling structure **12**.[31]

(23) Collman, J. P.; Hegedus, L. S.; Norton, J. R.; Finke, R. G. *Principles and Applications of Organotransition Metal Chemistry*, 2nd ed.; University Science Books: Mill Valley, CA, 1987; pp 241−244.

(24) The coordinated alcohol might be expected to possess distinctive spectroscopic properties (e.g., shifted ^{1}H NMR resonances for the benzylic protons, PhC*H*$_2$OH), but such evidence was not obtained, even at low temperatures. Such distinctions may not be evident, however, if the adduct is highly fluxional in the presence of a large excess of substrate.

(25) For recent studies and leading references on five-coordinate palladium(II) complexes, see: (a) Albano, V. G.; Natile, G.; Panunzi, A. *Coord. Chem. Rev.* **1994**, *133*, 67−114. (b) Di Bianca, F.; Bandoli, G.; Dolmella, A.; Antonaroli, S.; Crociani, B. *J. Chem. Soc., Dalton Trans.* **2002**, 212−217. (c) Fernández, D.; García-Seijo, M. I.; Kégl, T.; Petócz, G.; Kollár, L.; García-Fernández, M. E. *Inorg. Chem.* **2002**, *41*, 4435−4443. (d) Favez, R.; Roulet, R. *Inorg. Chem.* **1981**, *20*, 1598−1601.

(26) Cooper, J.; Ziegler, T. *Inorg. Chem.* **2002**, *41*, 6614−6622.

(27) Popp, B. V.; Landis, C. R.; Stahl, S. S. unpublished results. We have recently initiated a full computational analysis of "proton-coupled" ligand substitution reactions. Preliminary results relevant to the present system may be summarized as follows: Density functional theory (DFT) calculations, conducted with the B3[28a]-LYP[28b] functional and the LANL2DZ[28c−e] basis set with the Gaussian 98[28f] suite of programs, have been performed to optimize gas-phase geometries for each of the reactants and products in the equilibrium: **1** + $CH_3OH \leftrightarrow (py)_2Pd(OCH_3)(OAc) + AcOH$. The optimized structures were verified to be at a local minimum by calculation of the harmonic vibrational frequencies. Attempts to locate a stable five-coordinate palladium structures analogous to **9** and **10** have been unsuccessful. In each case, the optimization routine yields a minimum energy structure that possesses a hydrogen bond between the alcohol O−H and the carbonyl oxygen of a coordinated acetate ligand. The alcohol oxygen is oriented over the axial coordination site, but lies at a nonbonding distance of 3.6 Å. Relaxed potential energy surface (RPES) scans have also been conducted to probe the reaction pathway. The scans are conducted in the reverse (energetically favorable) direction by using optimized geometries of the square planar palladium-methoxide intermediate and acetic acid. The carbonyl oxygen of the acetic acid is directed over the axial coordination site of Pd, and the proton of the acid is directed over the oxygen of the methoxide ligand. Initial scans produce a product structure that closely resembles the optimized, hydrogen-bonded, alcohol adduct described above, which possesses no formal palladium−oxygen interaction. The transition state in this pathway has a trigonal bipyramidal structure in which the trigonal plane consists of two monodentate acetate ligands and an oxygen-bound alcohol ligand.

(28) (a) Becke, A. D. *Phys. Rev. A* **1988**, *38*, 3098−3100. (b) Lee, C.; Yang, W.; Parr, R. G. *Phys. Rev. B* **1988**, *37*, 785−789. (c) Hay, P. J.; Wadt, W. R. *J. Chem. Phys.* **1985**, *82*, 270−283. (d) Wadt, W. R.; Hay, P. J. *J. Chem. Phys.* **1985**, *82*, 284−298. (e) Hay, P. J.; Wadt, W. R. *J. Chem. Phys.* **1985**, *82*, 299−310. (f) Frisch, M. J.; Trucks, G. W.; Schlegel, H. B.; Scuseria, G. E.; Robb, M. A.; Cheeseman, J. R.; Zakrzewski, V. G.; Montgomery, J. A.; Stratmann, R. E.; Burant, J. C.; Dapprich, S.; Millam, J. M.; Daniels, A. D.; Kudin, K. N.; Strain, M. C.; Farkas, O.; Tomasi, J.; Barone, V.; Cossi, M.; Cammi, R.; Mennucci, B.; Pomelli, C.; Adamo, C.; Clifford, S.; Ochterski, J.; Petersson, G. A.; Ayala, P. Y.; Cui, Q.; Morokuma, K.; Salvador, P.; Dannenberg, J. J.; Malick, D. K.; Rabuck, A. D.; Raghavachari, K.; Foresman, J. B.; Cioslowski, J.; Ortiz, J. V.; Baboul, A. G.; Stefanov, B. B.; Liu, G.; Liashenko, A.; Piskorz, P.; Komaromi, I.; Gomperts, R.; Martin, R. L.; Fox, D. J.; Keith, T.; Al-Laham, M. A.; Peng, C. Y.; Nanayakkara, A.; Challacombe, M.; Gill, P. M. W.; Johnson, B.; Chen, W.; Wong, M. W.; Andres, J. L.; Gonzalez, C.; Head-Gordon, M.; Replogle, E. S.; Pople, J. A. *Gaussian 98*, revision A.10; Gaussian, Inc.: Pittsburgh, PA, 2001.

(29) (a) Mandal, S. K.; Jensen, D. R.; Pugsley, J. S.; Sigman, M. S. *J. Org. Chem.* **2003**, *68*, 4600−4603. (b) Bagdanoff, J. T.; Ferreira, E. M.; Stoltz, B. M. *Org. Lett.* **2003**, *5*, 835−837.

(30) A five-coordinate alcohol complex was proposed, but a structure analogous to **11**, in which the alcohol hydrogen bonds to a chloride ligand of [(−)-sparteine]PdCl$_2$, is also consistent with the experimental results.

(31) Sigman and co-workers have noted that [(−)-sparteine]Pd(OAc)$_2$ exhibits a background rate in the absence of exogenous base (ref 10b). Morever, they have recently reported a crystal structure of a palladium complex with acetate and water ligands in which the acetate engages in a six-membered ring intramolecular hydrogen bond (ref 10c).

Our kinetic results suggest that both neutral (pyridine) and anionic (acetate) ligands can promote reoxidation of palladium by molecular oxygen. If pyridine is excluded from the reaction mixture, no catalytic turnover is observed and palladium black forms rapidly. These observations reflect the direct competition between catalyst oxidation and decomposition upon formation of palladium(0) (Scheme 1). The beneficial role of pyridine can arise from stabilization of palladium(0) to prevent aggregation or from an enhanced reaction rate between palladium(0) and molecular oxygen. Both effects are probably important. Acetate appears to be capable of playing a similar role, when present in excess, because addition of NBu_4OAc to a reaction mixture lacking pyridine enables catalytic turnover (Figure 6). As with pyridine, it is not known whether this effect arises from stabilization of palladium(0) or enhancement of the oxygenation rate. A similar acetate effect was noted recently by Sheldon et al.,[9b] and the result is consistent with a series of recent studies that indicate anionic ligands promote oxidative addition of other substrates (e.g., aryl halides) to palladium(0).[32]

The beneficial effect of pyridine maximizes at a 1:1 py:Pd ratio. At higher concentrations, pyridine inhibits the reaction (Figure 5). The origin of this inhibition is evident upon consideration of the mechanism of β-hydride elimination. Square-planar metal alkyl and alkoxide complexes undergo β-hydride elimination through either three-[33] or four-coordinate[34,35] pathways. The former requires endergonic ligand dissociation prior to elimination, but this mechanism is generally preferred if a sufficiently labile ligand is coordinated to the metal. Complexes that undergo β-hydride elimination through a four-coordinate pathway often possess chelating ligands that hinder ligand dissociation.[34] The positive slope in the Hammett plot for substituted pyidines (Figure 12) is consistent with the expectation that electron-deficient pyridines should undergo more facile ligand dissociation. Meanwhile, nonlabile chelating ligands, such as 2,2′-bipyridine, strongly inhibit catalytic turnover.[12b] That the catalytic rate does not drop to zero at very high [pyridine] suggests elimination from a four-coordinate complex (**7**) is also possible; however, it occurs much more slowly than from the three-coordinate complex, **8**.

A rate law derived for this mechanism, based on preequilibrium formation of **1·RCH$_2$OH** and a steady-state approximation for intermediates **7** and **8**, is shown in eq 16.[36] As [$PhCH_2OH$] increases to the point of saturation and $K_1[PhCH_2OH] \gg 1$, the rate law simplifies to that shown in eq 17. The presence of [AcOH] and [py] in the denominator of this expression reflects their inhibitory effect on the reaction (Figures 5 and 7).

$$\frac{d[RCHO]}{dt} = \frac{K_1 k_2 k_3 k_4 [Pd]_T [PhCH_2OH]}{(1 + K_1[PhCH_2OH])(k_{-2}[AcOH](k_{-3}[py] + k_4) + k_3 k_4)} \quad (16)$$

$$\frac{d[RCHO]}{dt} = \frac{k_2 k_3 k_4 [Pd]_T}{k_{-2}[AcOH](k_{-3}[py] + k_4) + k_3 k_4} \quad (17)$$

The Origin of Nonlinear Rate Dependence on Catalyst Concentration. The toxicity and high cost of palladium have prompted considerable effort to develop more active palladium catalysts that can be used at lower catalyst loading.[37] The Pd(OAc)$_2$/pyridine-catalyzed alcohol oxidation exhibits significantly higher catalytic efficiency at lower catalyst loading. The turnover frequency is 9.4 h^{-1} at 10% catalyst loading, but increases nearly an order of magnitude to 90 h^{-1} at 0.2 mol % loading. The decrease in efficiency at higher catalyst loading is sufficiently severe that the absolute rate does not increase beyond 3 mol % catalyst loading (Figure 4). The mechanistic origin of this phenomenon has important implications for the development of improved oxidation catalysts.

The change in catalytic efficiency is revealed by a nonlinear dependence of the rate on the [catalyst] (Figure 4). Recently, such nonlinear kinetic behavior has been observed for two other palladium oxidation catalysts:[38] Sheldon's Pd(OAc)$_2$/bathophenanthroline sulfonate complex (**5**)[9a,b] and the Pd(OAc)$_2$/DMSO catalyst system.[8b] The origin of the nonlinear behavior differs in the two cases. In the aqueous alcohol oxidation reaction catalyzed by **5**, kinetic studies reveal a half-order dependence on the [catalyst]. Diimine-coordinated palladium and platinum complexes commonly form hydroxide-bridged dimers in aqueous solution.[39] This precedence together with the kinetics data suggest the catalyst resting state is a dimer, **(LPd^{II})$_2$**, that must break into a monomer to promote substrate oxidation (Scheme 4). The monomer−dimer equilibrium shifts toward a higher fraction of monomer at lower [catalyst] (see inset, Scheme 4), and, therefore, higher catalytic activity is observed at lower catalyst loading.

The nonlinear [catalyst] dependence in the Pd(OAc)$_2$/DMSO reaction has a different origin. The catalyst resting state in this case is palladium(0) rather than palladium(II). Our recent studies of this reaction[8b] reveal that catalyst aggregation and decomposition compete with the productive reaction between palladium(0) and molecular oxygen (Scheme 5). The rate of catalyst aggregation exhibits a bimolecular dependence on [palladium],

(32) (a) Amatore, C.; Jutand, A.; Thuilliez, A. *Organometallics* **2001**, *20*, 3241−3249. (b) Amatore, C.; Jutand, A. *Acc. Chem. Res.* **2000**, *33*, 314−321. (c) Amatore, C.; Jutand, A. *J. Organomet. Chem.* **1999**, *576*, 254−278. (d) Alcazar-Roman, L. M.; Hartwig, J. F. *J. Am. Chem. Soc.* **2001**, *123*, 12905−12906. (e) Alcazar-Roman, L. M.; Hartwig, J. F. *Organometallics* **2002**, *21*, 491−502.

(33) (a) Whitesides, G. M.; Gaasch, J. F.; Stedronsky, E. R. *J. Am. Chem. Soc.* **1972**, *94*, 5258−5270. (b) Alibrandi, G.; Minniti, D.; Romeo, R.; Cum, G.; Gallo, R. *J. Organomet. Chem.* **1985**, *291*, 133−137. (c) Romeo, R.; Alibrandi, G.; Scolaro, L. M. *Inorg. Chem.* **1993**, *32*, 4688−4694. (d) Goj, L. A.; Widenhoefer, R. A. *J. Am. Chem. Soc.* **2001**, *123*, 11133−11147. (e) Shultz, L. H.; Brookhart, M. *Organometallics* **2001**, *20*, 3975−3982. (f) Zhao, J.; Hesslink, H.; Hartwig, J. F. *J. Am. Chem. Soc.* **2001**, *123*, 7220−7227.

(34) (a) Bryndza, H. E. *J. Chem. Soc., Chem. Commun.* **1985**, 1696−1698. (b) Bryndza, H. E.; Calabrese, J. C.; Marsi, M.; Roe, D. C.; Tam, W.; Bercaw, J. E. *J. Am. Chem. Soc.* **1986**, *108*, 4805−4813. (c) Sacco, A.; Mastrorilli, P. *J. Chem. Soc., Dalton Trans.* **1994**, 2761−2764.

(35) (a) Ozawa, F.; Ito, T.; Yamamoto, A. *J. Am. Chem. Soc.* **1980**, *102*, 6457−6463. (b) Alibrandi, G.; Cusumano, M.; Minniti, D.; Scolaro, L. M.; Romeo, R. *Inorg. Chem.* **1989**, *28*, 342−347. (c) Alibrandi, G.; Scolaro, L. M.; Minniti, D.; Romeo, R. *Inorg. Chem.* **1990**, *29*, 3467−3472.

(36) A derivation of this rate law is provided in the Supporting Information. This mechanism and rate expression permits all of our kinetics data to be fit simultaneously in a self-consistent manner (Figure S14). Attempts to fit the [AcOH]-dependence data based on a mechanism with rapid equilibration of all intermediates (**1·RCH$_2$OH**, **7**, and **8**) prior to rate-limiting β-hydride elimination were unsuccessful.

(37) This goal has been especially evident in the development of palladium-catalyzed cross-coupling reactions. See, for example: (a) ref 2b. (b) Littke, A. F.; Fu, G. C. *Angew. Chem., Int. Ed.* **2002**, *41*, 4176−4211.

(38) Linear [catalyst] dependence has also been observed. See ref 10.

(39) (a) Wimmer, S.; Castan, P.; Wimmer, F. L.; Johnson, N. P. *Inorg. Chim. Acta* **1988**, *142*, 13−15. (b) Wimmer, S.; Castan, P.; Wimmer, F. L.; Johnson, N. P. *J. Chem. Soc., Dalton Trans.* **1989**, 403−412. (c) Fekl, U.; van Eldik, R.; Richardson, C.; Robinson, W. T. *Inorg. Chem.* **2001**, *40*, 3247−3251.

Scheme 4. Origin of Nonlinear [Catalyst] Dependence in the Aqueous Alcohol Oxidation Reaction Catalyzed by $Pd(OAc)_2$/Bathophenanthroline Sulfonate (**5**)

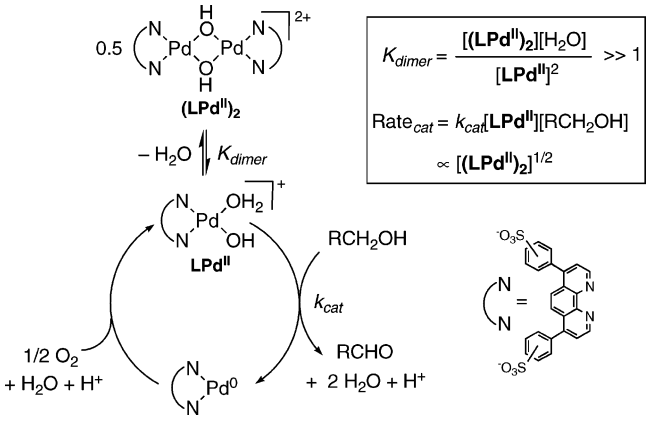

Scheme 5. Origin of Nonlinear [Catalyst] Dependence in Aerobic Alcohol Oxidation Catalyzed by the $Pd(OAc)_2$/DMSO System

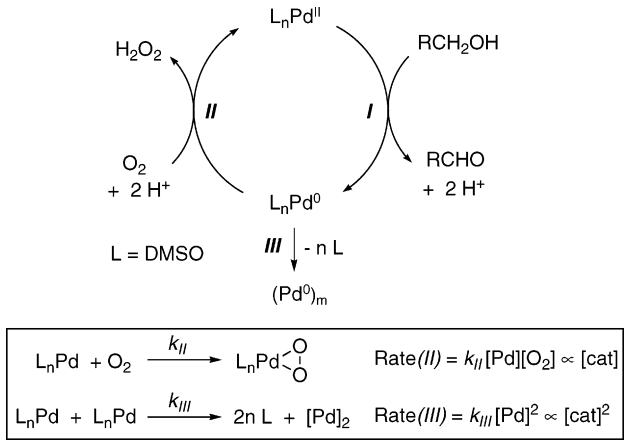

whereas catalytic turnover is unimolecular in [palladium]. The squared versus linear dependence of these processes on the [catalyst], respectively (inset, Scheme 5), dictates that productive catalytic turnover will experience a competitive advantage at lower catalyst loading and lead to higher efficiency.

In the $Pd(OAc)_2$/pyridine-catalyzed reaction, the catalyst concentration dependence varies under different reaction conditions. The dependence is hyperbolic when [catalyst] is varied at a constant 4:1 pyridine:$Pd(OAc)_2$ ratio (Figure 4), parabolic when [$Pd(OAc)_2$] is varied in the presence of constant excess [pyridine] (Figure 8A), and linear when [$Pd(OAc)_2$] is varied in the presence of constant [pyridine] and [AcOH] (Figure 8B). The previously characterized mechanisms (Schemes 4 and 5) do not explain these kinetic results. In situ spectroscopic study of the catalytic reaction reveals the catalyst resting state is monomeric in palladium, **1**/**1**·**RCH$_2$OH**, even in the presence of excess pyridine. The spectroscopic data also exclude catalyst decomposition, because the equilibrium mixture of **1** (together with **3** and **4** under certain conditions) and **1**·**RCH$_2$OH** account for all of the palladium added to the reaction mixture. Furthermore, no palladium black forms under standard reaction conditions. Therefore, catalyst aggregation, either as a dimer (Scheme 4) or decomposition into bulk palladium (Scheme 5), cannot account for the nonlinear behavior.

With the use of a gaseous substrate in these reactions, it was necessary to exclude the possibility that mass transfer of the oxygen into solution produces the nonlinear [catalyst] dependence.[40] The independence of the rate on both the oxygen pressure and the stirring rate rules out this explanation.

The proposed mechanism for palladium(II)-mediated alcohol oxidation (Scheme 3) provides an explanation for the variable [catalyst] dependence observed for the $Pd(OAc)_2$/pyridine system (Figures 4 and 8). The steady-state concentration of acetic acid and pyridine during the reaction will be proportional to the catalyst concentration, unless an excess of either component is added separately (see reaction conditions in Figure 8). Therefore, an increase in the catalyst loading will also increase the inhibitor concentration. Steps 2 and 3 of the mechanism (k_2 and k_3, Scheme 3) exhibit a first-order dependence on the catalyst concentration in the forward direction. Because pyridine and acetic acid are formed in equal concentration to intermediates **7** and **8**, respectively, the reverse steps (k_{-2} and k_{-3}) formally exhibit a bimolecular dependence on the catalyst concentration. Thus, at higher catalyst loading, the reverse steps will gain a competitive advantage over the forward steps. When excess pyridine is added to the reaction mixture, the [pyridine] no longer is proportional to the catalyst loading. Under these conditions, a half-order dependence on [$Pd(OAc)_2$] is observed (Figure 8A). Although this result could imply catalyst dimerization, in situ spectroscopic data do not support this conclusion. Instead, the half-order dependence arises from the competition between the unimolecular forward (k_2) and bimolecular reverse (k_{-2}) reactions in step 2 of the mechanism. (The k_{-2} step is formally bimolecular in [Pd] because [AcOH] = [**7**].) When excess [AcOH] and [pyridine] are both added to the reaction mixture, such that neither is proportional to the [catalyst], a first-order dependence on [$Pd(OAc)_2$] is observed (Figure 8B).

This analysis reveals that bimolecular or higher order catalyst side reactions (dimerization, Scheme 4; bulk aggregation, Scheme 5) are not necessary to produce a nonlinear [catalyst] dependence. Instead, the nonlinear behavior in the $Pd(OAc)_2$/pyridine reaction arises from a monomeric catalyst that undergoes competitive ligand dissociation and recombination (steps 2 and 3, Scheme 3). Attempts to increase catalyst activity by promoting facile ligand dissociation (e.g., electron-deficient pyridines) must be balanced by the need to prevent catalyst decomposition. Application of mechanistic principles such as these provides the basis for ongoing studies to develop new catalysts that exhibit high activity and may be used at low catalyst loading.

Summary

The $Pd(OAc)_2$/pyridine catalyst system has been applied to a variety of selective aerobic oxidation reactions, and this mechanistic study of benzyl alcohol oxidation provides insights into the factors that control catalyst activity and stability. We have, for the first time, complemented the kinetic study of an aerobic palladium-catalyzed oxidation reaction with direct spectroscopic characterization of the catalyst resting state. Such data facilitated elucidation of the detailed mechanism of palladium(II)-mediated alcohol oxidation and also revealed a

(40) (a) Albal, R. S.; Shah, Y. T.; Schumpe, A.; Carr, N. L. *Chem. Eng. J.* **1983**, *27*, 61−80. (b) Albal, R. S.; Shah, Y. T.; Carr, N. L.; Bell, A. T. *Chem. Eng. Sci.* **1984**, *39*, 905−907. (c) Deimling, A.; Karandikar, B. M.; Shah, Y. T.; Carr, N. L. *Chem. Eng. J.* **1984**, *29*, 127−140. (d) Sun, Y.; Landau, R. N.; Wang, J.; LeBlond, C.; Blackmond, D. G. *J. Am. Chem. Soc.* **1996**, *118*, 1348−1353.

new source of catalyst deactivation that can arise from the overoxidation of a primary alcohol to the carboxylic acid. The nonlinear rate dependence on the [catalyst] has a different origin than other palladium-catalyzed aerobic oxidation reactions, and analysis of this effect suggests new opportunities for the design of improved catalysts.

This study also highlights the complex, yet critical, role of ligands in modulating catalyst activity and stability. The neutral ligand, pyridine, plays a key role in the stabilization and aerobic oxidation of palladium(0), and we also obtained evidence that anionic ligands facilitate palladium(0) oxidation. The effect of pyridine on palladium(II)-mediated alcohol oxidation appears to be primarily inhibitory because it occupies a coordination site required for β-hydride elimination. Acetate participates directly in the formation of the palladium alkoxide, via initial hydrogen bond formation with the substrate and followed by proton-coupled ligand substitution. If this ligand is not sufficiently basic, formation of the palladium-alkoxide will be highly disfavored and reduce the catalyst activity. This principle has been detected in the $PdCl_2$/(−)-sparteine-catalyzed reactions where the anionic ligand, chloride, is sufficiently nonbasic that an exogenous base is required to achieve even stoichiometric alcohol oxidation.

Experimental Section

General Considerations. Palladium acetate (DuPont) was recrystallized prior to use from benzene/acetic acid.[41] Oxygen gas (BOC), benzyl alcohol (Aldrich), *para*-substituted alcohols (Aldrich), *sec*-phenethyl alcohol (Aldrich), pyridine (Aldrich), tetrabutylammonium acetate (Aldrich), sodium acetate (Aldrich), benzoic acid (Aldrich), benzaldehyde (Ruger), hexadecane (Aldrich), lithium aluminum deuteride (Aldrich), 1,3,5-tri-*tert*-butyl benzene (Aldrich), and pyridine (Aldrich) were used without purification. Benzyl alcohol-d_1, PhCH(D)OH, and benzyl alcohol-d_2, $PhCD_2OH$, were prepared by standard methods involving lithium aluminum deuteride reduction of benzaldehyde and benzoic acid. $(py)_2Pd(O_2CPh)_2$ was prepared by a literature procedure,[41] and crystals suitable for X-ray crystallographic analysis were obtained by evaporation of toluene. Toluene (Fisher) and diethyl ether (Fisher) were purified by passage through a column of activated alumina and Q4. Gas chromatographic analysis of reactions was conducted with a Shimadzu GC-17A gas chromatograph. ^{1}H NMR data were recorded using a Varian Inova (^{1}H: 500 MHz), a Varian Unity (^{1}H: 500 MHz), a Bruker AVANCE (^{1}H: 360 MHz), or a Bruker AC (^{1}H: 300 MHz) spectrometer. Spectra acquired at 80 °C were temperature calibrated with ethylene glycol. Chemical shifts were referenced to residual protons in the deuterated solvent, toluene-d_8: 2.09 ppm. 1,3,5-Tri-*tert*-butylbenzene was used as an internal standard for ^{1}H NMR spectral data (7.34 ppm, 1.32 ppm).

(41) Stephenson, T. A.; Morehouse, S. M.; Powell, A. R.; Heffer, J. P.; Wilkinson, G. *J. Chem. Soc.* **1965**, 3632−3640.

Gas-Uptake Kinetics. A typical reaction was conducted as follows. $Pd(OAc)_2$ (11.2 mg, 50 μmol) was added to a 25 mL round-bottom flask with a stirbar. A solution of pyridine (22.3 mM in toluene, 9.0 mL) was added to $Pd(OAc)_2$. The flask was attached to an apparatus with a calibrated volume and a pressure transducer designed to measure the gas pressure within the sealed reaction vessel. The apparatus was evacuated to 300 Torr and filled with oxygen to 900 Torr, and this cycle was repeated 10 times. The pressure was established at 700 Torr, and the flask was heated to 80 °C. When the pressure stabilized in the apparatus, benzyl alcohol (1.0 M in toluene, 1.0 mL) was added via syringe through a septum. Data were acquired using custom software written within LabVIEW (National Instruments). Correlations between oxygen uptake and conversion were made via analysis by gas chromatography with hexadecane as an internal standard.

Catalytic Reaction Monitored by NMR Spectroscopy. A freshly prepared solution of $Pd(OAc)_2$ and pyridine (5.79 mM palladium, 23.5 mM pyridine, 3.41 mM 1,3,5-tri-*tert*-butylbenzene, in toluene-d_8, 0.440 mL) was added to a medium-wall NMR tube (#524PP, Wilmad) attached to a sealed 14/20 ground glass joint. The solution was frozen in liquid nitrogen, and benzyl alcohol (1.40 M in toluene-d_8, 0.060 mL) was added to it. The NMR tube was connected to a gas manifold attached to a mercury monometer, both of which were calibrated for volume. The solution was degassed three times, and then oxygen (0.577 mmol) was condensed in the tube to achieve a final pressure of 10 atm in the headspace above the solution. The NMR tube was flame-sealed (gas volume = 1.66 mL), and the solution was kept cold in a bath of dry ice/acetone until it was inserted into the spectrometer probe, preheated to 80 °C.

Titrations Monitored by NMR Spectroscopy. A typical data set for benzyl alcohol is described as follows. A freshly prepared solution of $Pd(OAc)_2$ and pyridine (3.12 mM palladium, 20.0 mM pyridine, 3.25 mM 1,3,5-tri-*tert*-butylbenzene, in toluene-d_8, 1.000 mL) was added to an NMR tube. Toluene-d_8 (0.080 mL) was added to it. A solution of benzyl alcohol (5.0 M in toluene-d_8, 0.010 mL) was added to the catalyst solution seconds before inserting the tube into the spectrometer. Titration experiments varied the amount of toluene-d_8 and benzyl alcohol that were added, keeping their total volume at 0.090 mL.

Acknowledgment. This work was supported by the Dreyfus Foundation (New Faculty and Teacher-Scholar Award), the Sloan Foundation (Research Fellowship), and the NIH (RO1 GM67173-01). Funding for NMR instrumentation was provided by the NIH (1 S10 RR04981-01 and 1 S10 RR08389-01) and the NSF (CHE-8813550, CHE-9629688, CHE-9629688, CHE-9208463, and CHE-9709065).

Supporting Information Available: Additional figures, NMR spectra, and crystallographic data (PDF, CIF). This material is available free of charge via the Internet at http://pubs.acs.org.

JA049962M